Journal of
Computational and Theoretical Nanoscience
Vol. 2, 1–13, 2005

# Multilevel Quantum Chemistry Approach to the Development of a Database of the SAM-Ligand-Metal Ion-Protein Interactions

Bartosz Trzaskowski,[1,*] Andrzej Les,[1] Ludwik Adamowicz,[2]
Pierre A. Deymier,[3] Roberto Guzman,[4] and Stepan G. Stepanian[5]

[1] *Department of Chemistry, Warsaw University, Pasteura 1, 02-093 Warsaw, Poland*
[2] *Department of Chemistry,* [3] *Department of Material Science and Engineering, and*
[4] *Department of Chemical and Environmental Engineering, University of Arizona, Tucson, Arizona 85721, USA*
[5] *Institute for Low-Temperature Physics and Engineering, National Academy of Sciences of Ukraine, 47 Lenin Avenue, Kharkov 310164*

An *ab-initio* approach towards building a database of immobilized ligands targeting proteins is presented. Iminodiacetic chelators, precursors of self-assembled monolayers, attached to the gold surface and complexing three divalent metal ions (Cu(II), Zn(II), Ni(II)) is investigated. The strength of the protein–ligand interaction is estimated. Ten models of the iminodiacetic acid metal complex with different degree of complexity were constructed, each focusing on different structural features of the system. The calculations have been performed using the quantum mechanical density functional theory method. The results show that reduction of the complexity of the model by removing the gold surface, the neighboring alkyl chains and the presence of the solvent does not have much impact on the iminodiacetic acid—aminoacid affinity. The interaction between the chelator and the aminoacid represented by imidazole moiety of histidine are also almost unaffected by the length of the alkyl chain. The results indicate that advanced quantum mechanical methods and relatively small model systems can be used to adequately describe the self-assembled monolayer-ligand-metal ion-protein interactions and to create a comprehensive database of ligands for the monolayers.

**Keywords:** Self-Assembled Monolayers, Protein Immobilization, Chelator, Biosensors, DFT.

RESEARCH ARTICLE

## 1. INTRODUCTION AND MOTIVATION

Specific and effective attachment of various proteins and aminoacids to metallic interfaces is a subject of very extensive work nowadays. Most work in this field, which is important due to its applications in macromolecules crystallization and structure determination,[1–4] protein purifications,[5,6] protein, RNA and DNA immobilization,[7–9] synthesis of biopolymers,[10] as well as constructing nanoscale biosensors and electronic devices,[11–13] has been carried out on self-assembled monolayers (SAMs). Some of the most commonly used SAMs, such as those formed by alkyl chains attached to the gold surface using thiol groups, are experimentally well described systems.[14–18] Also the number of theoretical investigations of such systems is constantly increasing.[19–25]

SAMs of alkanethiolates on gold can be easily functionalized by numerous, diverse chemical moieties that target specific aminoacids. The most common way to prepare a protein-targeting a SAM is to use amine-terminated alkanethiols deposited on gold and to exchange some of the terminal $NH_2$ groups by metal chelating agents such as iminodiacetic acid (IDA)[3,26,27] or nitrilotriacetate (NTA).[5,6,28–30] Both IDA and NTA are known for binding numerous di- and trivalent ions, and both, after complexing metal ions, have high affinities towards specific aminoacids. By far the most known and used among those systems is IDA with Cu(II). This system has a very high

*Author to whom correspondence should be addressed.


1546-198X/2005/2/001/013 doi:10.1166/jctn.2005.217

affinity towards histidine and has been extensively used in the chromatography based on immobilization of metals due to their affinity to certain proteins,[31] as well as in other experimental techniques relying on immobilized proteins. NTA has also been extensively used with Ni(II) since the resulting system has a high affinity towards histidines on the protein surface or on the multihistidine tag.

When devising a system for protein targeting, one is not limited to the two ligands (IDA and NTA) or the two metal ions (Cu(II) and Ni(II)) mentioned above. There are other di- and trivalent ions forming complexes with IDA, NTA and other chelating ligands with known high affinity towards certain aminoacids. Ligands, such as Tris(2-aminoethyl)amine,[32] dipycolylamine,[33] ethylene diamine,[34] 2-mercaptoethylamine,[35] and others are known to chelate very well such metal ions as Co(II),[36] Cu(II),[36] Zn(II),[36] Ni(II),[36] Mn(II),[37] Fe(III),[38] Hg(II),[39] Pd(II).[40] Lately new systems with less common ions such as Rh(II),[41] Eu(II)[42] or lanthanides[43] were discovered to form complexes that can be used in chromatography and protein immobilization. Combinations of various chelating ligands with various ions can produce systems with high affinity towards one or more aminoacids, however, only a few such systems are in common use. This is partially due to very good results obtained when using IDA-Cu-histidine or NTA-Ni-multihistidine tags, but probably also due to limited data available for other chelating systems.

It is important to notice that the selectivity and the affinity of the chelator-protein interaction can be affected not only by the choice of the chelator and the metal ion, but also by the variation of the spacer arm, the ligand density, the concentration of the salt, and the competing agents, the structure of the immobilized protein, as well as other factors. However, the protein affinity towards a metal chelate depends most strongly on the metal ion involved in coordination with the chelating agent.

Until now there has been no attempt to quantitatively and comprehensively characterize the interactions between the mentioned systems and aminoacids despite the growing number of synthesized chelating complexes. The first attempt to create a database of combinations of chelating ligands with metal ions and to describe their affinity towards different aminoacids using theoretical methods is presented in this work. Devising the ligand-metal ion database and extending it to include new combinations of ligands and metal ions can facilitate formation of novel chelating systems more specifically targeting certain aminoacids. The database can also be useful in describing the ligands using different types of interactions involved in binding aminoacids. The database would serve as a useful tool allowing selection of specific chelating agents for specific types of applications. The quantitatively described interactions between ligands, metal ions, and aminoacids would help to select the best possible species for such different applications as protein purification using chromatography (where the ligand-metal ion-protein complexation should be reversible) and attaching biological substrates to inorganic electronic devices for sensing technologies (where the ligand-metal ion-protein interactions should be non-reversible). Also the description of the different ligands and their interactions with different aminoacids should allow prediction of novel protein targets offering high interaction selectivity.

## 2. MODELS AND COMPUTATIONAL DETAILS

Iminodiacetic acid (IDA) was chosen for the study, since it forms numerous complexes with many metal ions and has a high affinity towards histidine residues. Three metal ions widely used in experiments were chosen for this investigation. The are: Cu(II), Zn(II), Ni(II). For each metal ion, ten models were built (Fig. 1) with decreasing level of structural complexity. For each model a full geometry optimization was performed using a small or standard basis set followed by an energy calculation. To simplify the calculations, the histidine molecule was represented as an imidazole moiety. It was suggested that such simplification should have a minor impact on the calculated relative interaction energies and the geometrical parameters.[44] In order to compare ligand-metal ion-aminoacid affinities, the relative interaction energy, $E(\mathrm{int})$, between the chelator and the aminoacid was defined as $E(\mathrm{int}) = E(\mathrm{im}) - E(\mathrm{water})$,

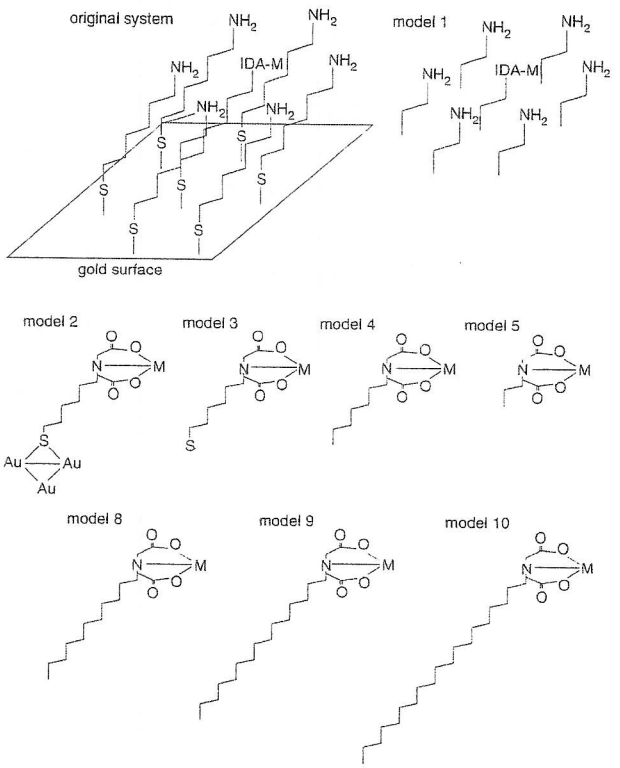


**Fig. 1.** Molecular models of ten affinity ligands used in the theoretical calculations as described in the Models and Computational Details section. M denotes a divalent metal ion.



RESEARCH ARTICLE

where $E$(im) is the energy of the interaction between the model system and imidazole and $E$(water) is the energy of the interaction between the model system and a water molecule.

The starting point for the modeling was a SAM system of amine-modified alkanethiols on the gold surface with some of the terminal $NH_2$ groups substituted by IDA (Fig. 1, see original system) and with the whole system placed in the water solution. Since the system is much too complex for DFT calculations, we tried to reduce its size and complexity, step by step, by removing some of its features to see if such changes influence the affinity of IDA ligand with the metal ion towards imidazole (Fig. 1). The final goal of the analysis was to find the smallest possible model which is suitable for density functional (DFT) calculations and simultaneously adequately represents the most essential geometrical and energetic features of the ligand-metal ion-aminoacid interaction.

In the model 1, we have reduced the system by removing the solvent and the entire gold surface, and by shortening the alkyl chain. The resulting system, with the terminal carbon atoms of the alkyl chain kept frozen in the process of the geometry optimization, was used to determine the influence of the neighboring amine groups on the IDA-imidazole complex. It was also used to study the influence of the bulky IDA group on the arrangement of the alkyl chains while completely neglecting thiol bonding to the gold surface and the water environment. All other models neglected the surrounding of the IDA-modified chain and describe only a single alkyl chain.

For model 1 we have performed partial structure optimization for the IDA-imidazole complex with the terminal carbon atoms of the alkyl chains frozen in the optimization. In the next step, the imidazole moiety was replaced by a water molecule using the average geometry for the IDA-water complex taken from the other models introduced in this work. The IDA-water interaction energy was evaluated by running partial optimization with the positions of both terminal carbon atoms of the alkyl chains and the water molecules fixed. In models 2–10, a full geometry optimizations of the systems were performed.

Model 2 included a seven-carbon alkyl chain attached through a thiol group to the $Au_3$ gold cluster. Such a cluster should provide a reasonable approximation of the gold surface in the calculation.[25] In the model the alkyl chain was modified by including an IDA group that interacts with a single imidazole moiety. In model 3 the gold cluster was removed, resulting in an unbound thiol group. The next step in reducing the complexity of the model is represented by model 4 in which the thiol group was removed, leaving a simple, unmodified alkyl chain. The last step of the reduction involved shortening of the alkyl chain from $C_7H_{15}$– to $C_3H_7$. This yielded model 5.

Since in models 1–5 the solution was completely neglected, two additional models were built. In model 6 (not illustrated), the solution was introduced using the PCM approach, which places the solute (model 5 in this case) in a cavity made of a series of overlapping spheres. In the second model, model 7 (not illustrated) the ligand system was placed within a highly-ordered cluster of 270 water molecules. As the starting geometry of the water cluster in that model we took a structure believed to correspond to a local minimum[45] with 10 water molecules removed and IDA-ion-imidazole model 5 put in their place.

Additional calculations were performed to check the influence of the alkyl chain length on the ligand-metal ion-protein interaction. Since most stable alkyl SAMs are formed by 7–19 carbon atom chains,[17,18] we used alkyl chains within this length range in our calculations. In the tests, we gradually modified model 4 by adding 4 (model 8), 8 (model 9), and 12 (model 10) —$CH_2$— groups to the alkyl chain.

For the geometry optimizations of model 2 through 10 the density functional DFT/B3LYP[46,47] method with the 6-31G* basis set for C, O, S, N, and H atoms, the VTZ[48] basis set for the first-row metal ions and the LANL2DZ[49,50] basis set for Au atoms were used. These calculations also yielded the total energies of the systems. Geometry of model 1 was optimized using the semiempirical PM3[51] method followed by a geometry optimization and an energy calculation at the B3LYP/6-31G*/VTZ level. We used the PCM model[52,53] for system 6 with water as the solvent. In model 7 we used the ONIOM method[54] in which the affinity ligand was placed in the inner layer and the water molecules were placed in the outer layer and were treated with the molecular mechanics method using the UFF force field.[55] For models 2–10 the hessian matrices were calculated in order to assess whether the predicted optimized geometries correspond to true minima. The zero-point energy corrections obtained in the hessian calculations were scaled by a factor of 0.96 and were added to the final molecular energies. The basis set superposition error (BSSE) correction was calculated using the Boys-Bernardi counterpoise scheme.[56]

The DFT and semiempirical PM3 calculations were performed using the quantum chemistry package Gaussian 03.[57]

## 3. RESULTS AND DISCUSSION

In this section, we discuss application of the proposed chelator models to study the IDA-Cu(II)-imidazole and IDA-Cu(II)-imidazole systems (Figs. 2 and 3). The results for systems with other metal ions (Zn(II), Ni(II)) are reported in the Supplementary Information section. We only refer to these other systems when their behavior differs from that of the IDA-Cu(II)-imidazole system.

Figures 4–8 show a comparison between crucial geometrical parameters, the relative interaction energies and

RESEARCH ARTICLE

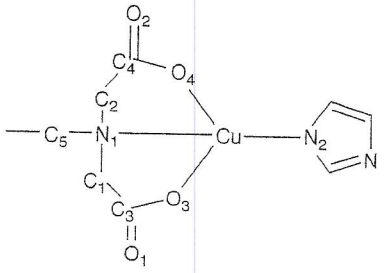


**Fig. 2.** The numbering scheme for the IDA-M-imidazole system used throughout this work. M stands for the metal ion: Cu(II), Zn(II) or Ni(II).

the Mulliken charges calculated for the proposed models. The results were used to check the reliability of the model in describing the IDA system. Since the goal of this work is to find the smallest possible model, we focus on model 5 which should be the most suitable for the DFT calculations. Detailed results for the IDA-Cu(II)-imidazole system and systems with other metal ions are reported in the Supplementary Information section.

The analysis of the geometrical features of models 1 to 10 immediately provides one important result: models 1, 6, and 7 are the only ones that show large differences in the crucial geometrical parameters of the chelator-aminoacid complex. For model 1 this is due to a number of features which can be found only in a non-isolated chains (Fig. 9). The IDA-Cu(II) group substituting one amine group distorts the local arrangement of the film by introducing a bulky molecular fragment and disallowing the formation of all possible hydrogen bonds between the terminal $NH_2$ groups. But the perturbation of the local arrangement is mutual because the nearby aminealkyl chains also have a non-negligible effect on the IDA chelator. The nearly planar structure of isolated IDA becomes distorted due to interaction between the utmost oxygen atoms of the chelator and the closest $NH_2$ groups. The orientation of the imidazole moiety towards IDA in the optimized structure differs from the case of nonsolvated models due to a sterical hindrance of other alkyl chains. The distortions resulting form the presence of the solvent and the hydrogen bonds connecting water molecules and the studied system are also present in models 6 and 7, described later.

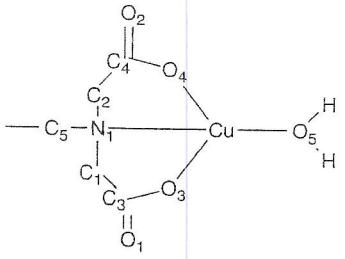


**Fig. 3.** The numbering scheme for IDA-M-water system used throughout this work. M stands for metal the ion: Cu(II), Zn(II) or Ni(II).

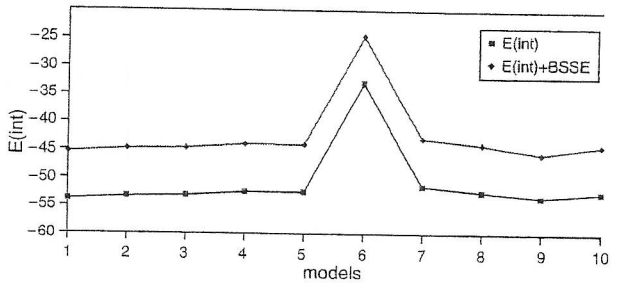


**Fig. 4.** Comparison of the energetics of the IDA-Cu(II)-imidazole interactions (in kJ/mol). Relative interaction energy E(int) was defined in the text.

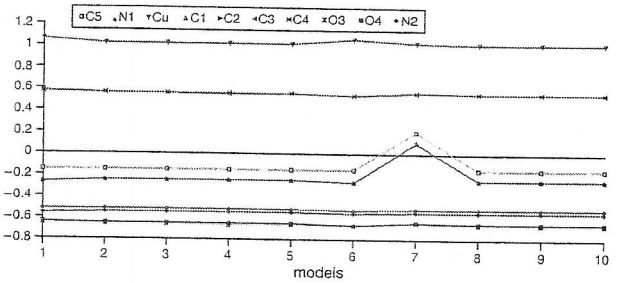


**Fig. 5.** Comparison of Mulliken charges on atoms of the IDA-Cu(II)-imidazole system depending on the model used.

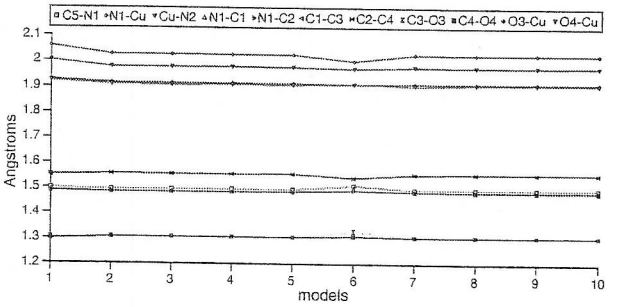


**Fig. 6.** Comparison of bond lengths of the IDA-Cu(II)-imidazole system depending on the model used.

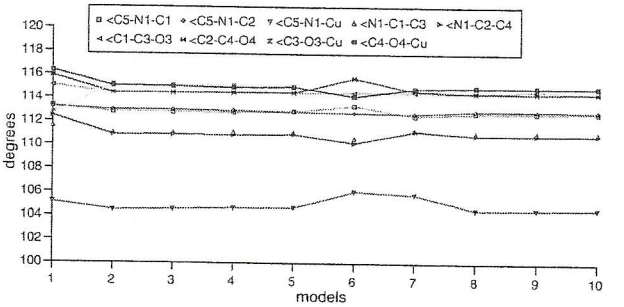


**Fig. 7.** Comparison of bond angles of the IDA-Cu(II)-imidazole system depending on the model used.



RESEARCH ARTICLE

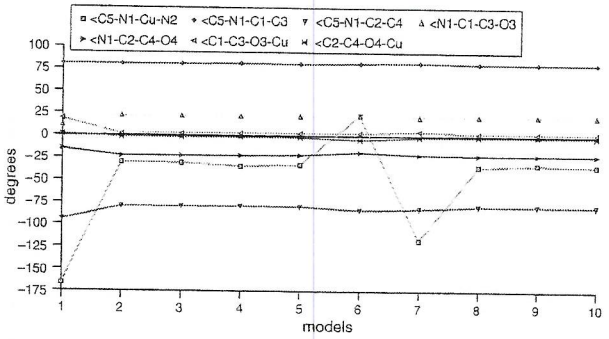


**Fig. 8.** Comparison of bond dihedral angles of the IDA-Cu(II)-imidazole system depending on the model used.

Although the neighboring alkyl chains have a relatively high impact on the geometrical and orientational features of the IDA-Cu(II) system, they do not have much influence on the relative energy of the ligand-metal ion-imidazole interaction (compare the results for models 1 through 5). These results and the similarity in the geometries of models 1–5 allow us to reduce the model to the simplest form (model 5) with minimal loss of information. This permits us to describe the chelator-aminoacid interactions quantitatively with less computational overhead. Moreover it is interesting to notice that there is a simple possibility of a partial elimination of the influence of neighboring alkyl chains on the chelator. This possibility requires that a new chelator system is introduced, which does not replace the terminal amine group of the alkanethiols, but instead attaches to it. This corresponds to the case of a film functionalization e.g., by tris(2-aminoethyl)amine (TREN) chelator (Fig. 10). In such a system, instead of replacing an $NH_2$ group (as IDA does), a short additional alkyl chain is attached to the $NH_2$ group of the alkyl chain by a short additional alkyl chain. The resulting system has an advantage over IDA since the chelating group sticks out of the film into the solution and is less distorted by the film surface. TREN may still influence the local arrangement of the alkyl chains on the gold surface, but possibly to a lesser extent than IDA.

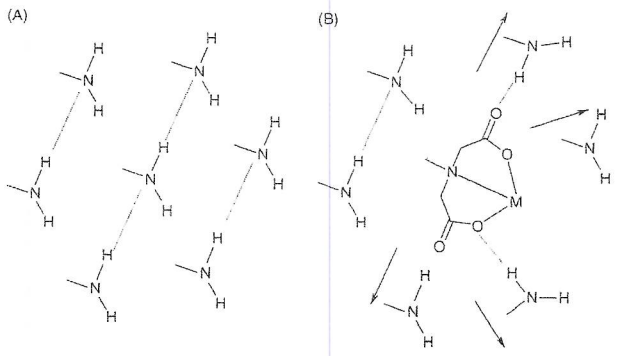


**Fig. 9.** Top view of an optimized geometry of amine-alkylthiols film (A) and model 1 (B). Dotted lines show possible hydrogen bonds. Black arrows show the relative change of the position of the terminal $NH_2$ groups of the alkyl chains due to the large volume of the IDA chelator.

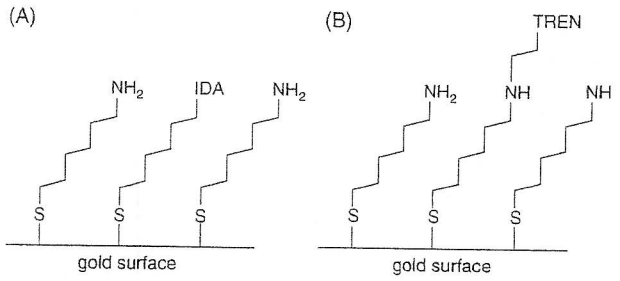


**Fig. 10.** Schematic view of an IDA-modified SAM (A) and a TREN-modified SAM on the gold surface (B).

It is important to notice that for model 1 and models with isolated alkyl chains the IDA-metal ion-imidazole interactions energies are not similar. This shows us that model 1, while introducing neighboring alkyl chains, still lacks some important features and fails to adequately describe the IDA system. The comparison of model 1 and other models gives us, however, a hint of possible problems that need to be overcome when devising more complex models describing global behavior of the SAM-ligand-metal ion-protein system.

Removing the neighboring alkyl chains is an event causing major structural adjustments in the described system. On the other hand, the chelating system behaves very similarly with and without gold surface or a cluster representing this surface in the calculations. Removing the gold cluster from model 2 yielding model 3 gives an identical IDA geometry within 0.1 Å in crucial bond lengths and a difference in the relative affinity energy of only 0.2 kJ/mol. This is a desirable behavior from the point of view of the simplicity of theoretical approach because including Au atoms in the model significantly rises the computational cost, even when using the DFT approach with smaller basis-sets such as the LANDL2DZ.

We do not suggest that the gold surface in SAMs is irrelevant to the geometry, the orientation or the behavior of the system. It is clear that metal surface is responsible for the certain arrangement of the alkyl chains, as well as their orientation on the surface. However, in the described system the terminal groups of the alkyl chains are most important elements of the structure of the system, and they are almost unaffected by the interaction with the gold surface. This is due to a relatively large distance between the IDA chelator and the closest gold atom, which is about 5.0 Å for the SAMs involving 7-carbon alkanethiols. The influence of the gold surface on the chelator is further diminished in the case of longer chains. It is probable that for very short alkyl chains this may not happen. SAMs constructed from short alkyl chains are, however, used in some applications and there are other problems there which have to be addressed,[58–62] which are beyond the scope of this work.

We can see similar behavior when removing thiol group from the alkyl chain. Systems with a –SH group (model 3)

RESEARCH ARTICLE

and without this moiety (model 4) are almost identical in terms of the geometry and the energetics of the terminal chelator group. The relative affinity energy difference between these models is only 0.7 kJ/mol and most structural parameters of IDA are nearly identical. The influence of the thiol group on IDA should also be diminished in longer IDA-modified alkyl chains.

At this point it is evident that the length of the model SAMs (and also likely the entire SAM) should not have much impact on the properties of the chelator attached to the terminal group of the alkyl chain. It is noticeable that the behavior and the properties of IDA complexing imidazole is almost independent of the length of the alkane in the range of 3 to 19 carbon atoms (models 4, 5, 8, 9, and 10). The difference between the IDA-affinity for those systems is within the standard error of the B3LYP method[63] and the crucial geometrical parameters are close to identical. This allows us to suggest that the same is probably also true for longer alkyl chains, although it is known that very long SAMs lose their high stability. The results (Tables I and II) allow us to use IDA with the shortest alkyl chain as a good model of the IDA-modified SAM on the gold surface.

It is also interesting to notice that the introduced models have a very similar basis set superposition error. We have calculated BSSE using the Boys-Bernardi counterpoise scheme for seven Cu systems (Table I); the results show that BSSE corrections for the models are identical within 0.1 kJ/mol. Due to this fact we have used the BSSE corrections calculated for Cu, Zn, and Ni systems using model 5 to modify the interaction energies of all other models.

Model 5 emerges as the simplest model and a good candidate for a template model for use in devising a database of combinations of chelating ligands with metal ions and their affinity towards different aminoacids. The comparison of the Mulliken charges (Fig. 5) suggest a very similar charge distribution within the described models. The only property of the real system of alkanethiols' SAMs on the gold surface not included in any of the foregoing models is the solvent. This problem is addressed in the calculations using models 6 and 7, which add two different representations of the solvent to model 5. Both models create a spherical solution cavity surrounding the chelator from all sides, which is somewhat inadequate because in the real system the penetration of the solvent below the SAMs surface is inhibited.

Model 7, which places the chelator system within a cluster of 270 water molecules treated at the molecular mechanics level during the calculations, provides some interesting results. There is a noticeable change in the geometry of IDA caused by the hydrogen bonds between water molecules and terminal oxygen atoms of the chelator. It is, however, important to notice that some of the oxygen atoms of IDA are in the real system already hydrogen-bonded to some terminal $NH_2$ groups of the modified alkyl chains (as in model 1). It implies that there is some competition between $NH_2$ and $H_2O$ in the formation of the hydrogen bonds and in the stabilization of the whole system. Despite all the geometrical differences between models 7 and 5, the relative interaction energies in these models are within 1.4 kJ/mol.

Introduction of the PCM method also has a non-negligible impact on geometry of model 5, but interestingly, it causes a major change of the affinity of the IDA-Cu(II) chelator towards imidazole. Analysis of the results for model 6 has to take into account the fact, that in this model the entire IDA system is placed within the cavity and surrounded by solvent. This is, however, not true on the SAM surface, where only a part of the IDA chelator is able to interact with the solvent and the rest of the molecule interacts only with the neighboring alkanethiols. Therefore we may assume that the single-molecule PCM model is not suitable for the correct description of the problem. The result for model 7, which represents the SAM in a more accurate manner, suggest on the other hand, that it is possible to get reliable results for the relative interaction energies and for the system geometries using model 5 without the presence of the solvent.

The immobilization of chelating compounds in the separation of metalloproteins has been used in chromatography for over 30 years;[31,64–72] there are many experimental data concerning the selectivity of various chelators involving different metal ions towards various aminoacids. In the case of IDA, the affinity of most proteins towards IDA is the highest for the Cu(II) system.[73] Using high-level theoretical approach and the molecular models with high degree of complexity, we are able to reproduce this dependency. The calculations are, however, very time-consuming. In this study, we obtained similar result for most molecular models introduced, including the simplest model 5 (Table II); the geometry of the chelator in this model is in agreement with the experimental geometry from the crystallographic data.[74] These results suggest that the DFT method and the models proposed in this work are valid and they facilitate an effective method of devising a theoretically-based database of

**Table I.** Comparison of the BSSE correction values for IDA-Cu systems (in kJ · mol).

| | IDA-Cu-imidazole | IDA-Cu-water |
|---|---|---|
| model 1 | — | — |
| model 2 | 31.19 | 22.86 |
| model 3 | 31.27 | 22.83 |
| model 4 | 31.29 | 22.82 |
| model 5 | 31.27 | 22.83 |
| model 6 | — | — |
| model 7 | — | — |
| model 8 | 31.19 | 22.81 |
| model 9 | 31.23 | 22.80 |
| model 10 | 31.21 | 22.85 |

**Table II.** Comparison of the BSSE uncorrected and corrected energetics of the relative IDA-histidine interactions for the simplest model used in the calculations (model 5) depending on the metal ion used (in kJ/mol).

| | Cu(II) | Zn(II) | Ni(II) |
|---|---|---|---|
| $E$(int) | −52.45 | −50.81 | −46.02 |
| $E$(int) + BSSE | −44.00 | −36.82 | −36.24 |

the SAM-ligand-metal ion-protein interactions despite the exclusion of many structural features and consideration of only a single alkyl chain.

## 4. CONCLUSIONS

Calculations of some selected ligand affinities towards imidazole using established theoretical approaches suggest that the proposed methodology of devising molecular database of SAM-ligand-metal ion-protein interactions produces adequate results. DFT calculations on IDA using relatively simple models suggest that the affinity of this chelator towards imidazole is the highest in the case of complexing with the Cu(II) ion, which is in agreement with the experimental data. They also suggest that in calculating properties of different combinations of SAM-chelator-metal ion-aminoacid systems one can almost completely neglect some of the structural features of the system and one can solely focus on the most important part, such as the one represented by model 5. This, due to the small size of the resulting system, allows the use of high-level *ab-initio* methods in obtaining quantitative information concerning the affinity of modified SAMs towards various aminoacids.

Some aspects of the system of interest, such as its global dynamics, cannot be described using the proposed approach; but based on the *ab-initio* calculations, parameters for modeling chelator-ion-aminoacid systems can be developed and adapted in molecular mechanics and molecular dynamics calculations. That would allow one to address the questions concerning the global behavior of the SAMs and to better characterize these systems using a combination of *ab-initio*, molecular mechanics and molecular dynamics methods.

## SUPPLEMENTARY INFORMATION

Comparison of the energetics, Mulliken charges and crucial geometrical parameters (models 1 through 10) are presented for the following systems: IDA-Cu(II)-imidazole, IDA-Cu(II)-water, IDA-Zn(II)-imidazole, IDA-Zn(II)-water, IDA-Ni(II)-imidazole, and IDA-Ni(II)-water.

**Table S.1.** Comparison of the BSSE corrected energetics of IDA-Cu(II)-imidazole interactions (in kJ/mol) and Mulliken charges on crucial atoms of the system depending on the model used. Relative interaction energy $E$(int) in kJ/mol was defined in the text.

| Atom | Model 1 | Model 2 | Model 3 | Model 4 | Model 5 | Model 6 | Model 7 | Model 8 | Model 9 | Model 10 |
|---|---|---|---|---|---|---|---|---|---|---|
| C5 | −0.15 | −0.15 | −0.15 | −0.15 | −0.15 | −0.15 | 0.20 | −0.15 | −0.15 | −0.15 |
| N1 | −0.52 | −0.52 | −0.52 | −0.52 | −0.52 | −0.53 | −0.52 | −0.52 | −0.52 | −0.52 |
| Cu | 1.06 | 1.02 | 1.02 | 1.02 | 1.02 | 1.06 | 1.03 | 1.02 | 1.02 | 1.02 |
| C1 | −0.26 | −0.25 | −0.25 | −0.25 | −0.25 | −0.27 | 0.11 | −0.25 | −0.25 | −0.25 |
| C2 | −0.27 | −0.25 | −0.25 | −0.25 | −0.25 | −0.27 | 0.10 | −0.25 | −0.25 | −0.25 |
| C3 | 0.58 | 0.56 | 0.56 | 0.55 | 0.56 | 0.54 | 0.56 | 0.56 | 0.56 | 0.56 |
| C4 | 0.57 | 0.56 | 0.56 | 0.56 | 0.56 | 0.54 | 0.57 | 0.56 | 0.56 | 0.56 |
| O3 | −0.65 | −0.66 | −0.66 | −0.67 | −0.66 | −0.67 | −0.64 | −0.66 | −0.66 | −0.66 |
| O4 | −0.64 | −0.65 | −0.65 | −0.65 | −0.65 | −0.67 | −0.64 | −0.65 | −0.65 | −0.65 |
| N2 | −0.56 | −0.55 | −0.55 | −0.55 | −0.55 | −0.56 | −0.55 | −0.55 | −0.55 | −0.55 |
| $E$(int) | −45.33 | −44.84 | −44.63 | −43.98 | −44.00 | −24.46 | −42.91 | −43.91 | −45.63 | −44.06 |

**Table S.2.** Comparison of most important geometrical parameters of IDA-Cu(II)-imidazole systems depending on model used in the calculations. Bond lengths are in Angstroms, bond angles and dihedral angles are in degrees.

| | Model 1 | Model 2 | Model 3 | Model 4 | Model 5 | Model 6 | Model 7 | Model 8 | Model 9 | Model 10 |
|---|---|---|---|---|---|---|---|---|---|---|
| bond | | | | | | | | | | |
| C5-N1 | 1.499 | 1.494 | 1.495 | 1.496 | 1.495 | 1.513 | 1.494 | 1.495 | 1.495 | 1.495 |
| N1-Cu | 2.058 | 2.026 | 2.026 | 2.025 | 2.025 | 2.005 | 2.027 | 2.025 | 2.025 | 2.025 |
| Cu-N2 | 2.002 | 1.975 | 1.975 | 1.976 | 1.975 | 1.968 | 1.976 | 1.975 | 1.975 | 1.976 |
| N1-C1 | 1.487 | 1.484 | 1.484 | 1.484 | 1.484 | 1.498 | 1.485 | 1.484 | 1.484 | 1.484 |
| N1-C2 | 1.488 | 1.484 | 1.484 | 1.484 | 1.485 | 1.492 | 1.485 | 1.484 | 1.484 | 1.485 |
| C1-C3 | 1.549 | 1.555 | 1.555 | 1.555 | 1.555 | 1.536 | 1.553 | 1.555 | 1.555 | 1.555 |
| C2-C4 | 1.552 | 1.556 | 1.555 | 1.555 | 1.556 | 1.538 | 1.555 | 1.556 | 1.556 | 1.556 |
| C3-O3 | 1.304 | 1.307 | 1.307 | 1.307 | 1.307 | 1.331 | 1.307 | 1.307 | 1.307 | 1.307 |
| C4-O4 | 1.299 | 1.307 | 1.307 | 1.307 | 1.307 | 1.305 | 1.306 | 1.307 | 1.307 | 1.307 |
| O3-Cu | 1.927 | 1.914 | 1.914 | 1.914 | 1.914 | 1.913 | 1.913 | 1.914 | 1.914 | 1.914 |
| O4-Cu | 1.922 | 1.908 | 1.907 | 1.908 | 1.907 | 1.913 | 1.904 | 1.908 | 1.908 | 1.908 |

continued...

**Table S.2.** continued.

| | Model 1 | Model 2 | Model 3 | Model 4 | Model 5 | Model 6 | Model 7 | Model 8 | Model 9 | Model 10 |
|---|---|---|---|---|---|---|---|---|---|---|
| angle | | | | | | | | | | |
| ⟨C5-N1-C1 | 113.30 | 112.78 | 112.76 | 112.74 | 112.85 | 113.34 | 112.50 | 112.74 | 112.75 | 112.77 |
| ⟨C5-N1-C2 | 113.22 | 112.96 | 112.96 | 112.92 | 112.83 | 112.75 | 112.70 | 112.95 | 112.94 | 112.92 |
| ⟨C5-N1-Cu | 105.12 | 104.45 | 104.53 | 104.65 | 104.66 | 106.09 | 105.85 | 104.55 | 104.57 | 104.61 |
| ⟨N1-C1-C3 | 111.55 | 111.00 | 111.04 | 111.09 | 111.06 | 110.57 | 111.25 | 111.07 | 111.08 | 111.10 |
| ⟨N1-C2-C4 | 112.42 | 110.85 | 110.87 | 110.85 | 110.93 | 110.18 | 111.23 | 110.89 | 110.89 | 110.90 |
| ⟨C1-C3-O3 | 115.02 | 114.40 | 114.42 | 114.46 | 114.43 | 114.48 | 114.48 | 114.46 | 114.64 | 114.47 |
| ⟨C2-C4-O4 | 115.87 | 114.39 | 114.42 | 114.42 | 114.47 | 115.70 | 114.61 | 114.44 | 114.44 | 114.45 |
| ⟨C3-O3-Cu | 112.63 | 115.11 | 115.05 | 115.03 | 114.97 | 114.15 | 114.82 | 115.00 | 115.00 | 114.99 |
| ⟨C4-O4-Cu | 116.30 | 115.01 | 114.97 | 114.89 | 114.96 | 114.14 | 114.84 | 114.93 | 114.92 | 114.91 |
| dihedral angle | | | | | | | | | | |
| ⟨C5-N1-Cu-N2 | −165.81 | −30.21 | −31.32 | −34.72 | −32.96 | 22.18 | −117.83 | −34.95 | −32.55 | −34.03 |
| ⟨C5-N1-C1-C3 | 80.22 | 80.31 | 80.44 | 80.91 | 80.48 | 80.93 | 81.67 | 80.63 | 80.69 | 80.76 |
| ⟨C5-N1-C2-C4 | −94.54 | −79.42 | −79.64 | −79.53 | −80.15 | −83.64 | −82.02 | −79.74 | −79.74 | −79.76 |
| ⟨N1-C1-C3-O3 | 11.59 | 22.09 | 21.78 | 21.43 | 21.65 | 22.26 | 20.46 | 21.45 | 21.43 | 21.41 |
| ⟨N1-C2-C4-O4 | −15.24 | −22.96 | −22.63 | −22.72 | −22.18 | −19.05 | −21.76 | −22.56 | −22.51 | −22.45 |
| ⟨C1-C3-O3-Cu | 18.58 | 1.80 | 2.23 | 2.40 | 2.55 | 2.75 | 4.36 | 2.53 | 2.54 | 2.54 |
| ⟨C2-C4-O4-Cu | 0.89 | −1.43 | −1.81 | −1.89 | −2.07 | −4.93 | −2.13 | −1.82 | −1.92 | −2.03 |

**Table S.3.** Comparison of Mulliken charges of IDA-Cu(II)-water on crucial atoms of the system depending on the model used.

| Atom | Model 1 | Model 2 | Model 3 | Model 4 | Model 5 | Model 6 | Model 7 | Model 8 | Model 9 | Model 10 |
|---|---|---|---|---|---|---|---|---|---|---|
| C5 | −0.16 | −0.16 | −0.16 | −0.16 | −0.15 | −0.15 | −0.15 | −0.16 | −0.16 | −0.16 |
| N1 | −0.54 | −0.54 | −0.54 | −0.54 | −0.54 | −0.55 | −0.53 | −0.54 | −0.54 | −0.54 |
| Cu | 1.08 | 1.03 | 1.03 | 1.03 | 1.03 | 1.06 | 1.03 | 1.03 | 1.03 | 1.03 |
| C1 | −0.26 | −0.25 | −0.25 | −0.25 | −0.25 | −0.29 | −0.25 | −0.25 | −0.25 | −0.25 |
| C2 | −0.27 | −0.25 | −0.25 | −0.25 | −0.25 | −0.27 | −0.25 | −0.25 | −0.25 | −0.25 |
| C3 | 0.58 | 0.57 | 0.57 | 0.57 | 0.57 | 0.54 | 0.57 | 0.57 | 0.57 | 0.57 |
| C4 | 0.58 | 0.57 | 0.57 | 0.57 | 0.57 | 0.54 | 0.57 | 0.57 | 0.57 | 0.57 |
| O3 | −0.65 | −0.67 | −0.67 | −0.67 | −0.67 | −0.68 | −0.67 | −0.67 | −0.67 | −0.67 |
| O4 | −0.66 | −0.67 | −0.67 | −0.67 | −0.67 | −0.68 | −0.66 | −0.67 | −0.67 | −0.67 |
| O5 | −0.81 | −0.81 | −0.81 | −0.81 | −0.81 | −0.85 | −0.81 | −0.81 | −0.81 | −0.81 |

**Table S.4.** Comparison of most important geometrical parameters of IDA-Cu(II)-water systems depending on model used in the calculations. Bond lengths are in Angstroms, bond angles and dihedral angles are in degrees.

| | Model 1 | Model 2 | Model 3 | Model 4 | Model 5 | Model 6 | Model 7 | Model 8 | Model 9 | Model 10 |
|---|---|---|---|---|---|---|---|---|---|---|
| bond | | | | | | | | | | |
| C5-N1 | 1.493 | 1.495 | 1.496 | 1.497 | 1.496 | 1.495 | 1.495 | 1.496 | 1.496 | 1.496 |
| N1-Cu | 2.018 | 2.006 | 2.005 | 2.004 | 2.004 | 1.997 | 2.004 | 2.004 | 2.004 | 2.004 |
| Cu-O5 | 2.053 | 2.024 | 2.024 | 2.025 | 2.025 | 2.018 | 2.009 | 2.025 | 2.025 | 2.025 |
| N1-C1 | 1.486 | 1.487 | 1.487 | 1.487 | 1.487 | 1.487 | 1.485 | 1.487 | 1.487 | 1.487 |
| N1-C2 | 1.489 | 1.487 | 1.487 | 1.487 | 1.487 | 1.487 | 1.486 | 1.487 | 1.487 | 1.487 |
| C1-C3 | 1.550 | 1.557 | 1.557 | 1.557 | 1.557 | 1.557 | 1.538 | 1.557 | 1.557 | 1.557 |
| C2-C4 | 1.555 | 1.557 | 1.557 | 1.557 | 1.557 | 1.557 | 1.538 | 1.557 | 1.557 | 1.557 |
| C3-O3 | 1.307 | 1.311 | 1.311 | 1.311 | 1.311 | 1.310 | 1.309 | 1.311 | 1.311 | 1.311 |
| C4-O4 | 1.301 | 1.311 | 1.311 | 1.311 | 1.311 | 1.310 | 1.305 | 1.311 | 1.311 | 1.311 |
| O3-Cu | 1.912 | 1.878 | 1.878 | 1.878 | 1.878 | 1.880 | 1.900 | 1.878 | 1.878 | 1.878 |
| O4-Cu | 1.905 | 1.878 | 1.878 | 1.878 | 1.878 | 1.880 | 1.901 | 1.878 | 1.878 | 1.878 |
| angle | | | | | | | | | | |
| ⟨C5-N1-C1 | 113.23 | 113.01 | 113.08 | 113.05 | 113.06 | 112.96 | 112.90 | 113.06 | 113.07 | 113.07 |
| ⟨C5-N1-C2 | 114.37 | 113.16 | 113.08 | 113.05 | 113.05 | 112.91 | 112.86 | 113.06 | 113.06 | 113.06 |
| ⟨C5-N1-Cu | 100.71 | 104.74 | 104.79 | 104.88 | 104.91 | 104.52 | 106.34 | 104.81 | 104.80 | 114.81 |
| ⟨N1-C1-C3 | 111.71 | 111.29 | 111.41 | 111.41 | 111.41 | 110.80 | 110.94 | 111.42 | 111.43 | 111.43 |
| ⟨N1-C2-C4 | 112.63 | 111.35 | 111.41 | 111.40 | 111.41 | 110.53 | 110.94 | 111.41 | 111.42 | 111.42 |
| ⟨C1-C3-O3 | 115.18 | 114.70 | 114.74 | 114.75 | 114.74 | 115.85 | 114.88 | 114.76 | 114.76 | 114.76 |
| ⟨C2-C4-O4 | 116.12 | 114.72 | 114.75 | 114.76 | 114.75 | 115.80 | 114.47 | 114.76 | 114.77 | 114.77 |
| ⟨C3-O3-Cu | 113.01 | 114.22 | 114.22 | 114.19 | 114.19 | 113.47 | 113.80 | 114.19 | 114.19 | 114.19 |
| ⟨C4-O4-Cu | 115.31 | 114.30 | 114.21 | 114.18 | 114.18 | 112.99 | 113.85 | 114.19 | 114.18 | 114.18 |

continued...

**Table S.4.** continued.

| | Model 1 | Model 2 | Model 3 | Model 4 | Model 5 | Model 6 | Model 7 | Model 8 | Model 9 | Model 10 |
|---|---|---|---|---|---|---|---|---|---|---|
| dihedral angle | | | | | | | | | | |
| ⟨C5-N1-Cu-O5 | −160.78 | 4.00 | −2.89 | −3.13 | −3.58 | −0.73 | −155.09 | −2.98 | −2.99 | −3.19 |
| ⟨C5-N1-C1-C3 | 80.05 | 81.96 | 82.67 | 82.79 | 82.75 | 85.02 | 81.78 | 82.78 | 82.80 | 82.82 |
| ⟨C5-N1-C2-C4 | −95.94 | −82.58 | −82.66 | −82.78 | −82.74 | −81.59 | −80.71 | −82.77 | −82.78 | −82.79 |
| ⟨N1-C1-C3-O3 | 10.43 | 21.33 | 21.09 | 21.04 | 21.12 | 19.77 | 22.33 | 20.93 | 20.88 | 20.87 |
| ⟨N1-C2-C4-O4 | −13.28 | −21.13 | −21.10 | −21.04 | −21.12 | −22.28 | −22.68 | −20.95 | −20.91 | −20.90 |
| ⟨C1-C3-O3-Cu | 15.20 | 1.46 | 1.18 | 1.23 | 1.17 | 2.94 | 1.94 | 1.31 | 1.36 | 1.38 |
| ⟨C2-C4-O4-Cu | 4.64 | −1.21 | −1.17 | −1.23 | −1.18 | −2.40 | −2.42 | −1.31 | −1.34 | −1.35 |

**Table S.5.** Comparison of the BSSE corrected energetics of IDA-Zn(II)-imidazole interactions (in kJ/mol) and Mulliken charges on crucial atoms of the system depending on the model used. Relative interaction energy $E$(int) was defined in the text.

| Atom | Model 1 | Model 2 | Model 3 | Model 4 | Model 5 | Model 6 | Model 7 | Model 8 | Model 9 | Model 10 |
|---|---|---|---|---|---|---|---|---|---|---|
| C5 | −0.16 | −0.16 | −0.16 | −0.16 | −0.15 | −0.16 | −0.15 | −0.16 | −0.16 | −0.16 |
| N1 | −0.54 | −0.57 | −0.57 | −0.57 | −0.57 | −0.57 | −0.55 | −0.58 | −0.58 | −0.58 |
| Zn | 1.44 | 1.39 | 1.40 | 1.40 | 1.39 | 1.42 | 1.37 | 1.40 | 1.40 | 1.40 |
| C1 | −0.25 | −0.24 | −0.24 | −0.24 | −0.24 | −0.27 | −0.25 | −0.24 | −0.24 | −0.24 |
| C2 | −0.27 | −0.25 | −0.24 | −0.24 | −0.24 | −0.28 | −0.25 | −0.24 | −0.24 | −0.24 |
| C3 | 0.58 | 0.55 | 0.55 | 0.55 | 0.55 | 0.53 | 0.55 | 0.55 | 0.55 | 0.55 |
| C4 | 0.56 | 0.55 | 0.55 | 0.55 | 0.55 | 0.53 | 0.55 | 0.55 | 0.55 | 0.55 |
| O3 | −0.70 | −0.73 | −0.73 | −0.73 | −0.73 | −0.69 | −0.73 | −0.73 | −0.73 | −0.73 |
| O4 | −0.71 | −0.73 | −0.73 | −0.73 | −0.73 | −0.70 | −0.73 | −0.73 | −0.73 | −0.73 |
| N2 | −0.61 | −0.64 | −0.64 | −0.64 | −0.64 | −0.71 | −0.63 | −0.64 | −0.64 | −0.64 |
| $E$(int) | −79.60 | −17.78 | −36.83 | −36.76 | −36.82 | −28.23 | −34.24 | −36.60 | −36.75 | −37.20 |

**Table S.6.** Comparison of most important geometrical parameters of IDA-Zn(II)-imidazole systems depending on model used in the calculations. Bond lengths are in Angstroms, bond angles and dihedral angles are in degrees.

| | Model 1 | Model 2 | Model 3 | Model 4 | Model 5 | Model 6 | Model 7 | Model 8 | Model 9 | Model 10 |
|---|---|---|---|---|---|---|---|---|---|---|
| bond | | | | | | | | | | |
| C5-N1 | 1.488 | 1.483 | 1.483 | 1.484 | 1.484 | 1.487 | 1.486 | 1.484 | 1.484 | 1.484 |
| N1-Zn | 2.212 | 2.145 | 2.144 | 2.141 | 2.143 | 2.135 | 2.164 | 2.141 | 2.140 | 2.140 |
| Zn-N2 | 2.095 | 2.018 | 2.017 | 2.018 | 2.018 | 2.010 | 2.027 | 2.018 | 2.018 | 2.017 |
| N1-C1 | 1.475 | 1.478 | 1.478 | 1.479 | 1.478 | 1.481 | 1.477 | 1.478 | 1.478 | 1.478 |
| N1-C2 | 1.480 | 1.479 | 1.479 | 1.479 | 1.479 | 1.478 | 1.477 | 1.479 | 1.479 | 1.479 |
| C1-C3 | 1.553 | 1.560 | 1.560 | 1.560 | 1.560 | 1.545 | 1.559 | 1.560 | 1.561 | 1.561 |
| C2-C4 | 1.560 | 1.562 | 1.562 | 1.562 | 1.562 | 1.545 | 1.560 | 1.562 | 1.562 | 1.562 |
| C3-O3 | 1.290 | 1.309 | 1.309 | 1.309 | 1.309 | 1.297 | 1.306 | 1.309 | 1.309 | 1.309 |
| C4-O4 | 1.294 | 1.308 | 1.308 | 1.308 | 1.308 | 1.294 | 1.305 | 1.308 | 1.308 | 1.309 |
| O3-Zn | 1.993 | 1.910 | 1.909 | 1.910 | 1.909 | 1.961 | 1.920 | 1.910 | 1.909 | 1.908 |
| O4-Zn | 1.948 | 1.894 | 1.894 | 1.895 | 1.895 | 1.944 | 1.907 | 1.894 | 1.895 | 1.895 |
| angle | | | | | | | | | | |
| ⟨C5-N1-C1 | 112.84 | 113.65 | 113.75 | 113.64 | 113.65 | 113.38 | 112.55 | 113.71 | 113.65 | 113.65 |
| ⟨C5-N1-C2 | 113.95 | 113.65 | 113.57 | 113.55 | 113.61 | 112.60 | 113.26 | 113.54 | 113.61 | 113.63 |
| ⟨C5-N1-Zn | 106.79 | 102.97 | 102.93 | 103.20 | 103.09 | 106.51 | 106.40 | 102.93 | 102.98 | 102.96 |
| ⟨N1-C1-C3 | 111.97 | 112.70 | 112.75 | 112.74 | 112.80 | 111.65 | 112.19 | 112.81 | 112.84 | 112.89 |
| ⟨N1-C2-C4 | 113.37 | 112.90 | 112.92 | 112.94 | 112.90 | 112.65 | 112.13 | 112.95 | 112.95 | 112.88 |
| ⟨C1-C3-O3 | 116.12 | 115.62 | 115.62 | 115.61 | 115.67 | 115.87 | 115.28 | 115.66 | 115.70 | 115.77 |
| ⟨C2-C4-O4 | 117.11 | 115.87 | 115.90 | 115.91 | 115.88 | 117.49 | 115.26 | 115.94 | 115.92 | 115.85 |
| ⟨C3-O3-Zn | 113.92 | 116.53 | 116.48 | 116.40 | 116.48 | 115.55 | 117.32 | 116.39 | 116.39 | 116.43 |
| ⟨C4-O4-Zn | 117.49 | 116.42 | 116.44 | 116.34 | 116.33 | 115.96 | 116.97 | 116.31 | 116.27 | 116.20 |
| dihedral angle | | | | | | | | | | |
| ⟨C5-N1-Zn-N2 | −165.89 | −5.47 | −5.23 | −5.13 | −5.47 | −15.07 | −38.52 | −5.50 | −5.26 | −5.46 |
| ⟨C5-N1-C1-C3 | 78.00 | 84.88 | 84.87 | 85.08 | 85.39 | 80.09 | 83.08 | 85.26 | 85.52 | 82.24 |
| ⟨C5-N1-C2-C4 | −95.84 | −84.62 | −84.96 | −85.23 | −84.75 | −92.44 | −81.68 | −85.09 | −84.92 | −84.09 |
| ⟨N1-C1-C3-O3 | 14.04 | 26.31 | 26.22 | 26.24 | 25.64 | 23.03 | 22.91 | 25.77 | 25.53 | 24.94 |
| ⟨N1-C2-C4-O4 | −7.89 | −24.36 | −23.99 | −23.90 | −24.42 | −15.28 | −25.81 | −23.76 | −24.00 | −24.59 |
| ⟨C1-C3-O3-Zn | 20.50 | −10.43 | −10.30 | −10.26 | −9.08 | 4.07 | 0.98 | −10.04 | −9.92 | −9.83 |
| ⟨C2-C4-O4-Zn | −12.12 | 7.21 | 7.07 | 6.90 | 7.31 | −2.87 | 1.83 | 6.90 | 6.98 | 7.01 |

RESEARCH ARTICLE

**Table S.7.** Comparison of Mulliken charges of IDA-Zn(II)-water on crucial atoms of the system depending on the model used.

| Atom | Model 1 | Model 2 | Model 3 | Model 4 | Model 5 | Model 6 | Model 7 | Model 8 | Model 9 | Model 10 |
|---|---|---|---|---|---|---|---|---|---|---|
| C5 | −0.18 | −0.16 | −0.16 | −0.15 | −0.15 | −0.15 | −0.15 | −0.16 | −0.16 | −0.16 |
| N1 | −0.56 | −0.59 | −0.59 | −0.59 | −0.59 | −0.60 | −0.58 | −0.59 | −0.59 | −0.59 |
| Zn | 1.41 | 1.37 | 1.37 | 1.37 | 1.37 | 1.43 | 1.37 | 1.37 | 1.37 | 1.37 |
| C1 | −0.24 | −0.25 | −0.25 | −0.25 | −0.25 | −0.29 | −0.25 | −0.25 | −0.25 | −0.25 |
| C2 | −0.27 | −0.25 | −0.25 | −0.25 | −0.25 | −0.27 | −0.25 | −0.25 | −0.25 | −0.25 |
| C3 | 0.56 | 0.56 | 0.56 | 0.56 | 0.56 | 0.53 | 0.55 | 0.56 | 0.56 | 0.56 |
| C4 | 0.57 | 0.56 | 0.56 | 0.56 | 0.56 | 0.53 | 0.56 | 0.56 | 0.56 | 0.56 |
| O3 | −0.71 | −0.75 | −0.74 | −0.75 | −0.75 | −0.75 | −0.74 | −0.74 | −0.74 | −0.75 |
| O4 | −0.71 | −0.74 | −0.74 | −0.75 | −0.74 | −0.74 | −0.74 | −0.75 | −0.75 | −0.74 |
| O5 | −0.79 | −0.85 | −0.85 | −0.85 | −0.85 | −0.89 | −0.85 | −0.85 | −0.85 | −0.86 |

**Table S.8.** Comparison of most important geometrical parameters of IDA-Zn(II)-water systems depending on model used in the calculations. Bond lengths are in Angstroms, bond angles and dihedral angles are in degrees.

| | Model 1 | Model 2 | Model 3 | Model 4 | Model 5 | Model 6 | Model 7 | Model 8 | Model 9 | Model 10 |
|---|---|---|---|---|---|---|---|---|---|---|
| bond | | | | | | | | | | |
| C5-N1 | 1.484 | 1.485 | 1.485 | 1.486 | 1.487 | 1.489 | 1.484 | 1.486 | 1.486 | 1.486 |
| N1-Zn | 2.197 | 2.130 | 2.128 | 2.127 | 2.128 | 2.114 | 2.133 | 2.126 | 2.125 | 2.125 |
| Zn-O5 | 2.262 | 2.092 | 2.092 | 2.093 | 2.094 | 2.050 | 2.092 | 2.093 | 2.094 | 2.100 |
| N1-C1 | 1.479 | 1.479 | 1.479 | 1.479 | 1.480 | 1.481 | 1.476 | 1.479 | 1.479 | 1.479 |
| N1-C2 | 1.482 | 1.479 | 1.479 | 1.479 | 1.480 | 1.480 | 1.477 | 1.479 | 1.479 | 1.480 |
| C1-C3 | 1.556 | 1.564 | 1.564 | 1.564 | 1.564 | 1.546 | 1.562 | 1.564 | 1.564 | 1.563 |
| C2-C4 | 1.555 | 1.565 | 1.564 | 1.564 | 1.564 | 1.547 | 1.563 | 1.564 | 1.564 | 1.565 |
| C3-O3 | 1.295 | 1.314 | 1.314 | 1.314 | 1.314 | 1.303 | 1.313 | 1.314 | 1.314 | 1.314 |
| C4-O4 | 1.299 | 1.314 | 1.314 | 1.314 | 1.314 | 1.301 | 1.313 | 1.314 | 1.314 | 1.315 |
| O3-Zn | 1.943 | 1.871 | 1.871 | 1.871 | 1.872 | 1.921 | 1.874 | 1.871 | 1.871 | 1.884 |
| O4-Zn | 1.909 | 1.870 | 1.871 | 1.871 | 1.872 | 1.920 | 1.870 | 1.872 | 1.871 | 1.863 |
| angle | | | | | | | | | | |
| ⟨C5-N1-C1 | 113.71 | 113.58 | 113.62 | 113.60 | 113.42 | 112.60 | 113.26 | 113.59 | 113.59 | 113.61 |
| ⟨C5-N1-C2 | 113.93 | 113.73 | 113.62 | 113.60 | 113.41 | 112.92 | 113.63 | 113.59 | 113.59 | 113.57 |
| ⟨C5-N1-Zn | 101.82 | 106.05 | 106.05 | 106.12 | 106.97 | 109.23 | 106.70 | 106.09 | 106.07 | 105.83 |
| ⟨N1-C1-C3 | 112.99 | 112.87 | 112.98 | 112.99 | 113.00 | 111.49 | 112.51 | 113.00 | 113.00 | 112.95 |
| ⟨N1-C2-C4 | 113.65 | 113.03 | 112.98 | 112.99 | 112.99 | 112.13 | 112.74 | 113.00 | 113.00 | 113.07 |
| ⟨C1-C3-O3 | 116.54 | 116.06 | 116.15 | 116.17 | 116.14 | 116.90 | 115.95 | 116.18 | 116.17 | 115.74 |
| ⟨C2-C4-O4 | 117.10 | 116.22 | 116.15 | 116.17 | 116.13 | 117.15 | 116.06 | 116.17 | 116.16 | 116.42 |
| ⟨C3-O3-Zn | 116.52 | 115.01 | 115.04 | 114.98 | 115.01 | 114.21 | 115.05 | 114.95 | 114.96 | 115.51 |
| ⟨C4-O4-Zn | 117.23 | 115.07 | 115.04 | 114.99 | 115.03 | 114.33 | 115.27 | 114.97 | 114.97 | 114.60 |
| dihedral angle | | | | | | | | | | |
| ⟨C5-N1-Zn-O5 | 141.24 | −0.92 | 0.11 | 0.12 | 0.73 | 12.44 | −22.02 | 0.45 | 0.44 | −24.06 |
| ⟨C5-N1-C1-C3 | 92.20 | 84.39 | 83.39 | 85.56 | 86.20 | 84.35 | 82.94 | 85.61 | 85.62 | 85.90 |
| ⟨C5-N1-C2-C4 | −94.76 | −85.94 | −85.40 | −85.56 | −86.21 | −87.76 | −85.12 | −85.62 | −85.63 | −85.40 |
| ⟨N1-C1-C3-O3 | 27.30 | 24.11 | 23.11 | 22.93 | 22.96 | 14.99 | 24.34 | 22.85 | 22.81 | 24.12 |
| ⟨N1-C2-C4-O4 | −2.39 | −22.71 | −23.11 | −22.93 | −22.96 | 32.34 | −21.87 | −22.86 | −22.83 | −22.41 |
| ⟨C1-C3-O3-Zn | −21.49 | −2.88 | −2.41 | −2.25 | −2.01 | 0.50 | −0.19 | −2.24 | −2.22 | −4.78 |
| ⟨C2-C4-O4-Zn | −15.07 | 2.34 | 2.42 | 2.26 | 2.02 | −0.81 | 0.17 | 2.27 | 2.25 | 1.72 |

**Table S.9.** Comparison of the BSSE corrected energetics of IDA-Ni(II)-imidazole interactions (in kJ/mol) and Mulliken charges on crucial atoms of the system depending on the model used. Relative interaction energy $E$(int) was defined in the text.

| atom | Model 1 | Model 2 | Model 3 | Model 4 | Model 5 | Model 6 | Model 7 | Model 8 | Model 9 | Model 10 |
|---|---|---|---|---|---|---|---|---|---|---|
| C5 | −0.15 | −0.16 | −0.16 | −0.16 | −0.16 | −0.17 | −0.16 | −0.16 | −0.16 | −0.16 |
| N1 | −0.52 | −0.53 | −0.53 | −0.53 | −0.53 | −0.55 | −0.53 | −0.53 | −0.53 | −0.53 |
| Ni | 1.26 | 1.16 | 1.16 | 1.16 | 1.16 | 1.22 | 1.15 | 1.15 | 1.16 | 1.15 |
| C1 | −0.27 | −0.25 | −0.24 | −0.24 | −0.25 | −0.28 | −0.25 | −0.25 | −0.25 | −0.25 |
| C2 | −0.27 | −0.25 | −0.25 | −0.25 | −0.25 | −0.28 | −0.25 | −0.25 | −0.25 | −0.25 |
| C3 | 0.58 | 0.56 | 0.56 | 0.56 | 0.56 | 0.53 | 0.56 | 0.56 | 0.56 | 0.56 |
| C4 | 0.55 | 0.56 | 0.56 | 0.56 | 0.56 | 0.54 | 0.56 | 0.56 | 0.56 | 0.56 |
| O3 | −0.68 | −0.69 | −0.69 | −0.69 | −0.69 | −0.69 | −0.69 | −0.69 | −0.69 | −0.69 |
| O4 | −0.66 | −0.68 | −0.68 | −0.68 | −0.68 | −0.69 | −0.68 | −0.68 | −0.68 | −0.68 |
| N2 | −0.57 | −0.57 | −0.57 | −0.57 | −0.57 | −0.59 | −0.57 | −0.57 | −0.57 | −0.57 |
| $E$(int) | −45.28 | −37.16 | −36.34 | −36.93 | −36.24 | −2.21 | −39.79 | −35.57 | −37.50 | −36.25 |

**Table S.10.** Comparison of most important geometrical parameters of IDA-Ni(II)-imidazole systems depending on model used in the calculations. Bond lengths are in Angstroms, bond angles and dihedral angles are in degrees.

| | Model 1 | Model 2 | Model 3 | Model 4 | Model 5 | Model 6 | Model 7 | Model 8 | Model 9 | Model 10 |
|---|---|---|---|---|---|---|---|---|---|---|
| bond | | | | | | | | | | |
| C5-N1 | 1.488 | 1.490 | 1.491 | 1.491 | 1.491 | 1.494 | 1.490 | 1.491 | 1.491 | 1.491 |
| N1-Ni | 2.139 | 2.073 | 2.072 | 2.071 | 2.072 | 2.047 | 2.067 | 2.066 | 2.070 | 2.066 |
| Ni-N2 | 2.043 | 2.007 | 2.007 | 2.008 | 2.008 | 1.992 | 2.004 | 2.007 | 2.008 | 2.007 |
| N1-C1 | 1.483 | 1.483 | 1.482 | 1.483 | 1.483 | 1.481 | 1.480 | 1.481 | 1.483 | 1.481 |
| N1-C2 | 1.488 | 1.483 | 1.483 | 1.483 | 1.483 | 1.482 | 1.480 | 1.481 | 1.483 | 1.481 |
| C1-C3 | 1.553 | 1.554 | 1.554 | 1.554 | 1.554 | 1.540 | 1.553 | 1.556 | 1.554 | 1.556 |
| C2-C4 | 1.561 | 1.554 | 1.555 | 1.554 | 1.554 | 1.540 | 1.552 | 1.556 | 1.554 | 1.556 |
| C3-O3 | 1.296 | 1.312 | 1.312 | 1.312 | 1.312 | 1.301 | 1.313 | 1.313 | 1.312 | 1.313 |
| C4-O4 | 1.291 | 1.312 | 1.312 | 1.312 | 1.312 | 1.302 | 1.313 | 1.313 | 1.312 | 1.313 |
| O3-Ni | 1.978 | 1.896 | 1.896 | 1.896 | 1.896 | 1.948 | 1.901 | 1.900 | 1.896 | 1.900 |
| O4-Ni | 1.957 | 1.889 | 1.889 | 1.889 | 1.889 | 1.938 | 1.891 | 1.892 | 1.889 | 1.893 |
| angle | | | | | | | | | | |
| ⟨C5-N1-C1 | 112.13 | 112.89 | 112.97 | 112.87 | 112.91 | 113.81 | 112.84 | 112.93 | 112.87 | 112.88 |
| ⟨C5-N1-C2 | 114.43 | 112.99 | 112.90 | 112.95 | 112.88 | 112.54 | 112.71 | 112.83 | 112.90 | 112.84 |
| ⟨C5-N1-Ni | 109.54 | 104.72 | 104.81 | 104.88 | 105.04 | 104.39 | 105.34 | 105.13 | 104.78 | 105.18 |
| ⟨N1-C1-C3 | 111.32 | 111.43 | 111.38 | 111.52 | 111.51 | 111.31 | 111.52 | 111.14 | 111.50 | 111.13 |
| ⟨N1-C2-C4 | 113.75 | 111.29 | 111.40 | 111.30 | 111.39 | 110.63 | 111.03 | 110.98 | 111.40 | 110.98 |
| ⟨C1-C3-O3 | 114.90 | 114.30 | 114.24 | 114.36 | 114.32 | 116.06 | 114.75 | 114.51 | 114.35 | 114.53 |
| ⟨C2-C4-O4 | 117.13 | 114.30 | 114.39 | 114.30 | 114.34 | 116.00 | 114.41 | 114.52 | 114.41 | 114.53 |
| ⟨C3-O3-Ni | 111.61 | 116.53 | 116.40 | 116.44 | 116.44 | 114.12 | 115.77 | 115.77 | 116.39 | 115.75 |
| ⟨C4-O4-Ni | 116.88 | 116.36 | 116.41 | 116.29 | 116.34 | 114.59 | 115.78 | 115.70 | 116.35 | 115.67 |
| dihedral angle | | | | | | | | | | |
| ⟨C5-N1-Ni-N2 | −135.63 | −18.21 | −16.70 | −17.50 | −17.19 | −35.56 | −52.89 | −33.14 | −16.41 | −32.62 |
| ⟨C5-N1-C1-C3 | 72.04 | 82.98 | 82.33 | 83.48 | 83.35 | 81.80 | 82.84 | 80.67 | 83.00 | 80.76 |
| ⟨C5-N1-C2-C4 | −117.64 | −80.21 | −82.96 | −82.24 | −82.79 | −81.84 | −79.86 | −79.96 | 83.02 | −80.01 |
| ⟨N1-C1-C3-O3 | 21.06 | 26.49 | 27.11 | 26.08 | 26.36 | 21.61 | 21.43 | 23.63 | 26.02 | 23.51 |
| ⟨N1-C2-C4-O4 | −10.24 | −27.36 | −26.45 | −27.32 | −26.90 | −18.82 | −24.76 | −24.49 | −26.36 | −24.41 |
| ⟨C1-C3-O3-Ni | 17.30 | −7.07 | −7.24 | −6.80 | −6.89 | 1.61 | 1.68 | 0.31 | −6.32 | 0.44 |
| ⟨C2-C4-O4-Ni | 12.13 | 7.38 | 6.91 | 7.40 | 7.17 | −5.40 | 0.45 | 0.34 | 6.88 | 0.19 |

**Table S.11.** Comparison of Mulliken charges of IDA-Ni(II)-water on crucial atoms of the system depending on the model used.

| Atom | Model 1 | Model 2 | Model 3 | Model 4 | Model 5 | Model 6 | Model 7 | Model 8 | Model 9 | Model 10 |
|---|---|---|---|---|---|---|---|---|---|---|
| C5 | −0.15 | −0.16 | −0.16 | −0.16 | −0.16 | −0.16 | −0.16 | −0.16 | −0.16 | −0.16 |
| N1 | −0.54 | −0.55 | −0.55 | −0.55 | −0.55 | −0.56 | −0.54 | −0.55 | −0.55 | −0.55 |
| Ni | 1.24 | 1.16 | 1.16 | 1.16 | 1.15 | 1.18 | 1.15 | 1.15 | 1.15 | 1.15 |
| C1 | −0.26 | −0.25 | −0.25 | −0.25 | −0.25 | −0.30 | −0.25 | −0.25 | −0.25 | −0.25 |
| C2 | −0.27 | −0.25 | −0.25 | −0.25 | −0.25 | −0.28 | −0.25 | −0.25 | −0.25 | −0.25 |
| C3 | 0.57 | 0.56 | 0.56 | 0.56 | 0.56 | 0.54 | 0.57 | 0.56 | 0.56 | 0.56 |
| C4 | 0.55 | 0.56 | 0.56 | 0.56 | 0.56 | 0.54 | 0.57 | 0.56 | 0.56 | 0.56 |
| O3 | −0.69 | −0.70 | −0.70 | −0.70 | −0.70 | −0.71 | −0.68 | −0.70 | −0.70 | −0.70 |
| O4 | −0.66 | −0.70 | −0.70 | −0.70 | −0.70 | −0.71 | −0.70 | −0.70 | −0.70 | −0.70 |
| O5 | −0.83 | −0.82 | −0.82 | −0.82 | −0.82 | −0.87 | −0.83 | −0.82 | −0.82 | −0.82 |

**Table S.12.** Comparison of most important geometrical parameters of IDA-Ni(II)-water systems depending on model used in the calculations. Bond lengths are in Angstroms, bond angles and dihedral angles are in degrees.

| | Model 1 | Model 2 | Model 3 | Model 4 | Model 5 | Model 6 | Model 7 | Model 8 | Model 9 | Model 10 |
|---|---|---|---|---|---|---|---|---|---|---|
| bond | | | | | | | | | | |
| C5-N1 | 1.486 | 1.491 | 1.492 | 1.492 | 1.492 | 1.494 | 1.490 | 1.492 | 1.492 | 1.492 |
| N1-Ni | 2.094 | 2.049 | 2.049 | 2.047 | 2.048 | 2.034 | 2.040 | 2.047 | 2.047 | 2.047 |
| Ni-O5 | 2.090 | 2.058 | 2.058 | 2.059 | 2.059 | 2.031 | 2.047 | 2.059 | 2.059 | 2.059 |
| N1-C1 | 1.486 | 1.487 | 1.487 | 1.487 | 1.487 | 1.488 | 1.481 | 1.487 | 1.487 | 1.487 |
| N1-C2 | 1.489 | 1.487 | 1.487 | 1.487 | 1.487 | 1.488 | 1.481 | 1.487 | 1.487 | 1.487 |
| C1-C3 | 1.548 | 1.555 | 1.555 | 1.555 | 1.555 | 1.535 | 1.557 | 1.555 | 1.555 | 1.555 |
| C2-C4 | 1.560 | 1.555 | 1.555 | 1.555 | 1.555 | 1.536 | 1.557 | 1.555 | 1.555 | 1.555 |
| C3-O3 | 1.304 | 1.317 | 1.317 | 1.317 | 1.317 | 1.313 | 1.318 | 1.317 | 1.317 | 1.317 |
| C4-O4 | 1.294 | 1.317 | 1.317 | 1.317 | 1.317 | 1.312 | 1.319 | 1.317 | 1.317 | 1.317 |
| O3-Ni | 1.935 | 1.861 | 1.861 | 1.861 | 1.861 | 1.892 | 1.863 | 1.861 | 1.861 | 1.861 |
| O4-Ni | 1.943 | 1.861 | 1.861 | 1.861 | 1.861 | 1.891 | 1.864 | 1.861 | 1.861 | 1.86 |

continued...

**Table S.12.** continued.

| | Model 1 | Model 2 | Model 3 | Model 4 | Model 5 | Model 6 | Model 7 | Model 8 | Model 9 | Model 10 |
|---|---|---|---|---|---|---|---|---|---|---|
| angle | | | | | | | | | | |
| ⟨C5-N1-C1 | 113.05 | 113.07 | 113.11 | 113.11 | 113.08 | 113.07 | 112.43 | 113.09 | 113.09 | 113.08 |
| ⟨C5-N1-C2 | 114.65 | 113.19 | 113.11 | 113.10 | 113.08 | 112.75 | 113.00 | 113.09 | 113.09 | 113.08 |
| ⟨C5-N1-Ni | 107.36 | 105.71 | 105.80 | 105.80 | 105.91 | 107.28 | 106.94 | 105.82 | 105.84 | 105.85 |
| ⟨N1-C1-C3 | 112.03 | 112.14 | 112.16 | 112.22 | 112.18 | 110.95 | 110.80 | 112.17 | 112.18 | 112.18 |
| ⟨N1-C2-C4 | 113.55 | 112.14 | 112.16 | 112.18 | 112.18 | 111.25 | 110.82 | 112.17 | 112.17 | 112.17 |
| ⟨C1-C3-O3 | 114.18 | 114.66 | 114.68 | 114.73 | 114.69 | 116.20 | 114.57 | 114.70 | 114.69 | 114.69 |
| ⟨C2-C4-O4 | 116.88 | 114.66 | 114.68 | 114.70 | 114.68 | 116.20 | 114.63 | 114.69 | 114.69 | 114.69 |
| ⟨C3-O3-Ni | 115.41 | 115.33 | 115.33 | 115.30 | 115.31 | 114.16 | 114.50 | 115.29 | 115.29 | 115.29 |
| ⟨C4-O4-Ni | 114.99 | 115.35 | 115.32 | 115.28 | 115.31 | 113.87 | 114.39 | 115.29 | 115.29 | 115.29 |
| dihedral angle | | | | | | | | | | |
| ⟨C5-N1-Ni-O5 | −125.14 | 0.95 | −0.40 | −1.01 | −0.04 | 41.29 | −130.68 | −0.36 | −0.28 | −0.34 |
| ⟨C5-N1-C1-C3 | 78.53 | 87.02 | 87.23 | 87.67 | 87.44 | 86.65 | 80.62 | 87.38 | 87.39 | 87.39 |
| ⟨C5-N1-C2-C4 | −128.57 | −87.07 | −87.21 | −87.28 | −87.40 | −85.79 | −80.78 | −87.34 | −87.35 | −87.37 |
| ⟨N1-C1-C3-O3 | 30.11 | 25.39 | 25.27 | 24.77 | 25.13 | 23.65 | 26.08 | 25.10 | 25.11 | 25.10 |
| ⟨N1-C2-C4-O4 | −1.94 | −25.34 | −25.28 | −25.05 | −25.15 | −22.95 | −25.33 | −25.13 | −25.13 | −25.11 |
| ⟨C1-C3-O3-Ni | −4.89 | −8.73 | −8.64 | −8.33 | −8.53 | −3.41 | −1.72 | −8.52 | −8.52 | −8.51 |
| ⟨C2-C4-O4-Ni | 15.32 | 8.64 | 8.63 | 8.37 | 8.52 | 1.72 | 0.49 | 8.53 | 8.52 | 8.50 |

**Acknowledgment:** CPU time provided in part by the Interdisciplinary Centre for Mathematical and Computational Modelling Center in Warsaw is gratefully acknowledged.

## References


1. S. A. Darst, H. O. Ribi, D. W. Pierce, and R. D. Kornberg, *J. Mol. Biol.* 203, 269 (**1988**).
2. R. Kornberg and S. A. Darst, *Curr. Opin. Struct. Biol.* 1, 642 (**1991**).
3. W. Frey, W. R. Schief, Jr., D. W. Pack, C.-T. Chen, A. Chilkoti, P. Stayton, V. Vogel, and F. H. Arnold, *Proc. Natl. Acad. Sci. USA* 93, 4937 (**1996**).
4. W. Frey, J. Brink, W. R. Schief, Jr., W. Chiu, and V. Vogel, *Biophys. J.* 74, 2674 (**1998**).
5. S. F. J. Le Grice and F. Gruninger-Leitch, *Eur. J. Biochem.* 187, 307 (**1990**).
6. R. Janknecht, G. de Martynoff, J. Lou, R. A. Hipskind, A. Nordheim, and H. G. Stunnenberg, *Proc. Natl. Acad. Sci. USA* 88, 8972 (**1991**).
7. C. R. Ill, V. M. Keivens, J. E. Hale, K. K. Nakamura, R. A. Jue, S. Cheng, E. D. Melcher, B. Drake, and M. C. Smith, *Biophys. J.* 64, 919 (**1993**).
8. A. Cricenti, S. Selci, A. C. Felici, R. Generosi, E. Gori, W. Djaczenko, and G. Charotti, *Science* 245, 1226 (**1989**).
9. X. Zhuang, L. E. Bartley, H. P. Babcock, R. Russell, T. Ha, D. Herschlag, and S. Chu, *Science* 288, 2048 (**2000**).
10. J. Li and W. J. Kao, *Biomacromolecules* 4, 1055 (**2003**).
11. M. A. Reed, C. Zhou, C. J. Muller, T. P. Burgin, and J. M. Tour, *Science* 278, 252 (**1997**).
12. J. Chen, M. A. Reed, A. M. Rawlett, and J. M. Tour, *Science* 286, 1550 (**1999**).
13. Z. J. Donhauser, B. A. Mantooth, K. F. Kelly, L. A. Bumm, J. D. Monnell, J. J. Stapleton, D. W. Price, Jr., A. M. Rawlett, D. L. Allara, J. M. Tour, and P. S. Weiss, *Science* 292, 2303 (**2001**).
14. C. D. Bain, E. B. Troughton, Y.-T. Tao, J. Evall, G. M. Whitesides, and R. G. Nuzzo, *J. Am. Chem. Soc.* 111, 321 (**1989**).
15. M. Buck, F. Eisert, J. Fischer, M. Grunze, and F. Trager, *Appl. Phys.* A53, 552 (**1991**).
16. H. A. Biebuyck, C. D. Bain, and G. M. Whitesides, *Langmuir* 10, 1825 (**1994**).
17. A. Ulman, *Chem. Rev.* 96, 1533 (**1996**).
18. G. E. Poirier, *Chem. Rev.* 97, 1117 (**1997**).
19. H. Sellers, A. Ulman, Y. Shnidman, and J. E. Eilers, *J. Am. Chem. Soc.* 115, 9389 (**1993**).
20. H. Gronbeck, A. Curioni, and W. Andreoni, *J. Am. Chem. Soc.* 122, 3839 (**2000**).
21. D. Kruger, H. Fuchs, R. Rousseau, D. Marx, and M. Parrinello, *J. Chem. Phys.* 115, 4776 (**2001**).
22. S. Jang, *Mol. Phys.* 100, 2261 (**2002**).
23. D. Fischer, A. Curioni, and W. Andreoni, *Langmuir* 19, 3567 (**2003**).
24. H. Basch and M. A. Ratner, *J. Chem. Phys.* 119, 11926 (**2003**).
25. C. Majumder, H. Mizuseki, and Y. Kawazoe, *J. Chem. Phys.* 118, 9809 (**2003**).
26. D. R. Shnek, D. W. Pack, D. Y. Sasaki, and F. H. Arnold, *Langmuir* 10, 2382 (**1994**).
27. D. Vancan, E. A. Miranda, and S. M. A. Bueno, *Process Biochem.* 37, 573 (**2002**).
28. B. Loddenkotter, B. Kammerer, K. Fischer, and U. Flugge, *Proc. Natl. Acad. Sci. USA* 90, 2155 (**1993**).
29. Ng. Kingman, D. W. Pack, D. Y. Sasaki, and F. H. Arnold, *Langmuir* 11, 4048 (**1995**).
30. J. Maly, C. Di Meo, M. De Francesco, A. Masci, J. Masojidek, M. Sugiura, A. Volpe, and R. Pilloton, *Bioelectrochemistry* 63, 271 (**2004**).
31. J. Porath, J. Carlsson, I. Olsson, and G. Belfrage, *Nature* 258, 598 (**1975**).
32. P. C. Jain and E. C. Lingafelter, *J. Am. Chem. Soc.* 89, 724 (**1967**).
33. A. D. Gupta and F. S. Richardson, *Inorg. Chem.* 20, 2616 (**1981**).
34. I. Garcia, M. Solache-Rios, P. Bosch, and S. Bulbulian, *Langmuir* 12, 4474 (**1996**).
35. R. E. DeSimone, T. Ontko, L. Wardman, and E. L. Blinn, *Inorg. Chem.* 14, 1313 (**1975**).
36. R. J. Sundberg and B. B. Martin, *Chem. Rev.* 74, 471 (**1974**).
37. E. J. Laskowski and D. N. Hendrickson, *Inorg. Chem.* 17, 457 (**1978**).
38. E. Sinn, G. Sim, E. V. Dose, M. F. Tweedle, and L. J. Wilson, *J. Am. Chem. Soc.* 100, 3375 (**1978**).
39. R. E. Bluhm, R. G. Bobbitt, L. W. Welch, A. J. Wood, J. F. Bonfiglio, C. Sarzen, A. J. Heath, and R. A. Branch, *Hum. Exp. Toxicol.* 11, 201 (**1992**).
40. M. A. Bennett, C. Chiraratvatana, G. B. Robertson, and U. Tooptakong, *Organometallics* 7, 1403 (**1988**).
41. N. C. Mosch-Zanetti, S. Kopke, R. Herbst-Irmer, and M. Hewitt, *Inorg. Chem.* 41, 3513 (**2002**).

42. P. Starynowicz, *Polyhedron* 22, 2761 (**2003**).
43. Q.-D. Liu, S. Gao, J.-R. Li, B.-Q. Ma, Q.-Z. Zhou, and K.-B. Yu, *Polyhedron* 21, 1097 (**2002**).
44. M. R. A. Blomberg, P. E. M. Siegbahn, G. T. Babcock, and M. J. Wikstrom, *Inorg. Biochem.* 80, 261 (**2000**).
45. M. F. Chaplin, *Biophys. Chem.* 83, 211 (**2000**).
46. A. D. Becke, *J. Chem. Phys.* 98, 5648 (**1993**).
47. C. Lee, W. Yang, and R. G. Parr, *Phys. Rev. B* 37, 785 (**1988**).
48. A. Schafer, H. Horn, and R. Ahlrichs, *J. Chem. Phys.* 97, 2571 (**1992**).
49. T. H. Dunning, Jr. and P. J. Hay, in Methods of Electronic Structure, Theory edited by H. F. Schaefer III, Plenum Press (**1977**), Vol. 3, p. 1.
50. P. J. Hay and W. R. Wadt, *J. Chem. Phys.* 82, 270 (**1985**).
51. J. J. P. Stewart, *J. Comp. Chem.* 10, 209 (**1989**).
52. S. Miertus, E. Scrocco, and J. Tomasi, *Chem. Phys.* 55, 117 (**1981**).
53. S. Miertus and J. Tomasi, *Chem. Phys.* 65, 239 (**1982**).
54. F. Maseras and K. Morokuma, *J. Comp. Chem.* 16, 1170 (**1995**).
55. A. K. Rappé, C. J. Casewit, K. S. Colwell, W. A. Goddard III, and W. M. Skiff, *J. Am. Chem. Soc.* 114, 10024 (**1992**).
56. S. B. Boys and F. Bernardi, *Mol. Phys.* 19, 553 (**1970**).
57. M. J. Frisch, G. W. Trucks, H. B. Schlegel, G. E. Scuseria, M. A. Robb, J. R. Cheeseman, J. A. Montgomery, Jr., T. Vreven, K. N. Kudin, J. C. Burant, J. M. Millam, S. S. Iyengar, J. Tomasi, V. Barone, B. Mennucci, M. Cossi, G. Scalmani, N. Rega, G. A. Petersson, H. Nakatsuji, M. Hada, M. Ehara, K. Toyota, R. Fukuda, J. Hasegawa, M. Ishida, T. Nakajima, Y. Honda, O. Kitao, H. Nakai, M. Klene, X. Li, J. E. Knox, H. P. Hratchian, J. B. Cross, C. Adamo, J. Jaramillo, R. Gomperts, R. E. Stratmann, O. Yazyev, A. J. Austin, R. Cammi, C. Pomelli, J. W. Ochterski, P. Y. Ayala, K. Morokuma, G. A. Voth, P. Salvador, J. J. Dannenberg, V. G. Zakrzewski, S. Dapprich, A. D. Daniels, M. C. Strain, O. Farkas, D. K. Malick, A. D. Rabuck, K. Raghavachari, J. B. Foresman, J. V. Ortiz, Q. Cui, A. G. Baboul, S. Clifford, J. Cioslowski, B. B. Stefanov, G. Liu, A. Liashenko, P. Piskorz, I. Komaromi, R. L. Martin, D. J. Fox, T. Keith, M. A. Al-Laham, C. Y. Peng, A. Nanayakkara, M. Challacombe, P. M. W. Gill, B. Johnson, W. Chen, M. W. Wong, C. Gonzalez, and J. A. Pople, Gaussian 03, Revision B.05, Gaussian, Inc., Pittsburgh PA (**2003**).
58. M. Tsen and L. Sun, *Anal. Chim. Acta* 307, 333 (**1995**).
59. J. Li, G. Cheng, and S. Dong, *J. Electroanal. Chem.* 416, 97 (**1996**).
60. M. H. Schoenfisch and J. E. Pemberton, *Langmuir* 15, 509 (**1999**).
61. V. Kertesz, N. A. Whittemore, G. B. Inamati, M. Manoharan, P. D. Cook, D. C. Baker, and J. Q. Chambers, *Electroanalysis* 12, 889 (**2000**).
62. A. Kudelski, *Langmuir* 19, 3805 (**2003**).
63. L. A. Curtis, K. Raghavachari, G. W. Trucks, and J. A. Pople, *J. Chem. Phys.* 94, 7221 (**1991**).
64. R. J. Everson and H. E. Parker, *Bioinorg. Chem.* 4, 15 (**1974**).
65. J. Porath and B. Olin, *Biochemistry* 22, 1621 (**1983**).
66. N. Ramadan and J. Porath, *J. Chromatogr.* 321, 93 (**1985**).
67. E. S. Hemdan, Y. J. Zhao, E. Sulkowski, and J. Porath, *Proc. Natl. Acad. Sci. USA* 86, 1811 (**1989**).
68. J. Porath, *Protein Expression Purif.* 3, 263 (**1992**).
69. E. Sulkowski, *Trends Biotechnol.* 3, 1 (**1985**).
70. E. Sulkowski, *Bioessays* 10, 170 (**1989**).
71. E. Sulkowski, *J. Mol. Recognit.* 9, 389 (**1996**).
72. E. Sulkowski, *J. Mol. Recognit.* 9, 494 (**1996**).
73. V. Gaberc-Porekar and V. Menart, *J. Biochem. Biophys. Methods* 49, 335 (**2001**).
74. A. Podder, J. K. Dattagupta, N. N. Saha, and W. Saenger, *Acta Cryst.* B35, 53 (**1979**).


Received: 30 March 2005. Accepted: 3 June 2005.

RESEARCH ARTICLE